BAREKENG: Journal of Mathematics and Its Applications
December 2025 Volume 19 Issue 4 Page 2777–2790
P-ISSN: 1978-7227 E-ISSN: 2615-3017
https://doi.org/10.30598/barekengvol19iss4pp2777-2790

BREAKING BARRIERS IN OPTIMIZATION: CHAOTIC MAP-INTEGRATED ALGORITHMS FOR PRACTICAL CHALLENGE

Pongchanun Luangpaiboon [1], Danupun Visuwan [2], Atiwat Nanphang [3], Lakkana Ruekkasaem [4*], Pasura Aungkulanon [5]

[1,2,3]*Industrial Statistics and Operational Research Unit (ISO-RU), Department of Industrial Engineering, Faculty of Engineering, Thammasat School of Engineering, Thammasat University*
[4]*Department of Mathematics and Statistics, Faculty of Science and Technology, Thammasat University Pathumthani, 12120, Thailand.*

[5]*Department of Materials Handling and Logistics Engineering, Faculty of Engineering, King Mongkut's University of Technology North Bangkok Bangkok, 10800, Thailand.*

*Corresponding author's e-mail: * **lakkana@mathstat.sci.tu.ac.th***

Article History:

Received: 25th February 2025
Revised: 19th April 2025
Accepted: 13th May 2025
Available online: 1st September 2025

Keywords:

Chaotic Maps;
Constraint Handling;
Metaheuristic Optimization;
Noisy Response Surfaces;
Rider Optimization Algorithm (ROA).
.

ABSTRACT

Real-world applications frequently necessitate optimization of chaotic response surfaces and constrained functions, which present difficult challenges for conventional methods. In order to effectively manage constraints and uncertainty, these complexities necessitate sophisticated algorithms. The objective of this research is to optimize the Rider Optimization Algorithm (ROA) by incorporating chaotic maps—namely, Logistic, Sinusoidal, and Iterative—to enhance exploration and exploitation. The chaotic ROA consistently outperforms the standard ROA in convergence speed, accuracy, and robustness, as evidenced by benchmark evaluations. For instance, in the multiple disk clutch brake design problem, the chaotic ROA obtained the highest objective value of 0.2352, which was equivalent to or greater than the leading algorithms TSO, MFO, and WOA. The chaotic ROA variants (ROAC1, ROAC2, ROAC3) exhibited superior stability by achieving low standard deviations (e.g., 0.3321 in the Branin function at high noise levels) across noisy response surface benchmarks. The integration of constraint-handling mechanisms guaranteed that practicable solutions were achieved without sacrificing optimality. The chaotic ROA is established as a robust and adaptable solution for complex, noisy, and constrained optimization challenges in industrial scheduling, resource allocation, and engineering design by the proposed approach.

How to cite this article:

P. Luangpaiboon, D. Visuwan, A. Nanphang, L. Ruekkasaem, and P. Aungkulanon, "BREAKING BARRIERS IN OPTIMIZATION: CHAOTIC MAP-INTEGRATED ALGORITHMS FOR PRACTICAL CHALLENGE", *BAREKENG: J. Math. & App.*, vol. 19, iss. 4, pp. 2777-2790, December, 2025.

Journal homepage: *https://ojs3.unpatti.ac.id/index.php/barekeng/*
Journal e-mail: *barekeng.math@yahoo.com; barekeng.journal@mail.unpatti.ac.id*

Research Article · Open Access

1. INTRODUCTION

Nature-inspired optimization algorithms have attracted considerable interest in recent decades for their efficacy in addressing complicated, nonlinear, and multimodal optimization challenges. Metaheuristic algorithms, including the Rider Optimization Algorithm (ROA) [1], have exhibited significant potential. ROA, informed by the operational conduct of entities, provides a distinctive framework to equilibrate exploration and exploitation, rendering it appropriate for diverse complex optimization challenges. Nonetheless, the efficacy of these methods may be compromised when utilized in noisy or limited optimization scenarios. The incorporation of chaotic maps into optimization algorithms has proven to be an effective method for improving their performance. Chaotic maps, originating from deterministic nonlinear systems, have characteristics including ergodicity, sensitivity to initial conditions, and randomness. This makes them effective for expanding the search space and averting premature convergence. Incorporating chaotic maps into metaheuristic algorithms enhances their convergence speed, solution precision, and robustness [2], [3]. This work investigates the synergistic potential of chaotic maps combined with ROA to tackle optimization issues defined by noisy response surfaces and constraints.

Noisy response surface optimization introduces uncertainty that can obscure the true landscape of the objective function, making it difficult for conventional optimization techniques to navigate effectively and frequently resulting in suboptimal solutions. The ROA is enhanced in its capacity to locate optimal solutions in noisy environments by incorporating chaotic maps, which improve its ability to manage uncertainties. Furthermore, the search for viable solutions can be substantially complicated by the presence of constraints in optimization problems, which can result in a reduction in the feasible search space. In order to overcome these obstacles, this investigation integrates constraint-handling techniques into the chaotic map-enhanced ROA framework, which allows the algorithm to maintain feasibility while pursuing optimality. This work advances metaheuristic optimization by integrating chaotic dynamics with ROA, thereby improving exploration, exploitation, and resilience beyond the capabilities of conventional methods in the presence of uncertainty and constraint limitations. The integration of constraint-handling techniques to balance feasibility and optimality in constrained problems, the development of a chaotic map-enhanced ROA to mitigate premature convergence and increase solution diversity, and a comprehensive comparative analysis using benchmark functions to evaluate the proposed algorithm against standard ROA and state-of-the-art methods are among the key contributions. The findings emphasize the benefits and constraints of incorporating chaos theory into metaheuristic optimization, providing valuable insights for practical applications in engineering, scheduling, and machine learning.

By means of benchmark trials on normal test functions, this study intends to assess and compare the efficacy of the ROA enhanced with chaotic maps in addressing noisy and constrained optimization challenges by determining the optimal method in terms of convergence speed, accuracy, resilience, and constraint-handling efficiency. It makes a major contribution to the field by means of creative integration of chaotic maps with ROA, thorough comparative analysis emphasizing the advantages and drawbacks of these advanced techniques, and inclusion of strong constraint-handling strategies to guarantee solution viability in constrained environments. With the paper organized to review ROA and chaotic maps, detail the methodology and experimental setup, present findings and analysis, and conclude with key insights and future research recommendations, the paper clarifies the role of chaotic maps in enhancing metaheuristic algorithms, establishes a foundation for future advancements, and demonstrates practical applications in many sectors including engineering design, resource allocation, machine learning, scheduling, supply chain management, and robust parameter estimation.

2. RESEARCH METHODS

2.1 Literature Review

Recent studies have demonstrated the transformative impact of hybrid optimization algorithms across diverse domains. Askarali and Fredrik [1] introduced an Enhanced Crow Search and Rider Optimization Algorithm for diagnosing spinal tuberculosis from CT images with 86% accuracy, while Roopa et al. [4] proposed a Chaotic Rider Optimization-Based Clustering Protocol to enhance energy efficiency and security in wireless sensor networks. Kumbhare et al. [5] leveraged a Federated Learning framework combined with a Hybrid Dragon-Rider Optimization Algorithm for breast cancer detection, achieving 95% accuracy, and

Sarangi et al. [6] developed the Exploitation-Assisted Driving Training-Rider Optimization (EDT-RO) model for multicast routing in MANETs to optimize QoS metrics. Addressing energy efficiency in IoT-enabled WBANs, Dinesh and Rangaraj [7] integrated a fuzzy logic system with a Modified Rider Optimization Algorithm, while Alazab et al. [8] introduced the Fitness Averaged Rider Optimization Algorithm for cluster head selection in IoT networks, targeting delay minimization and energy sustainability. Prasad and Jaya [9] developed an Adaptive Rider Optimization Algorithm for efficient spectrum sharing in Cognitive Radio Networks, and Deelip and Govinda [10] presented an Exponential Sunflower Rider Optimization Algorithm-driven deep residual network for IoT-based plant disease monitoring.

In secure drone communication, Raja et al. [11] employed ROA for deep learning-based image encryption to ensure optimal key generation, while Xu and Li [12] explored an Improved Whale Optimization Algorithm for uncertain utility portfolio optimization in financial markets. Further advancing hybrid strategies, Benghazouani et al. [13] combined WOA with other nature-inspired techniques for feature selection in breast cancer diagnosis, and Chen et al. [14] introduced the Competition of Tribes and Cooperation of Members Algorithm, demonstrating superior global optimization compared to WOA. Mehmood et al. [2] applied chaotic maps integrated with Atom Search Optimization for modeling electro-hydraulic actuator systems, and Roeva and Zoteva [3] enhanced chaotic electromagnetic field optimization using ten chaotic maps. Alibeigi et al. [15] employed deep learning and machine learning approaches, integrating hybrid models like DNN-GOA and SVR-WOA, to optimize high-temperature proton exchange membrane fuel cells with errors below 6%, while Palaniappan and Subramaniam [16] developed a WOA-based optimization model with response surface methodology to improve turning process parameters for mild steel.

Rajamani et al. [17] demonstrated multi-response optimization of plasma arc cutting parameters for Monel 400 alloys using WOA, and Kalita et al. [18] compared metaheuristic algorithms, including the Non-Dominated Sorting WOA, for Pareto optimization in wire electrical discharge machining. Kawecka [19] applied WOA to optimize parameters in abrasive water jet machining of tool steel, and Kumar et al. [20] utilized a hybrid ANN-WOA model for parametric optimization in fused deposition modeling, reducing surface roughness and production time. Finally, Liu et al. [21] introduced a quantum theory-based improved WOA to predict seismic responses in short structures by optimizing an ANN, thereby capturing complex structural behaviors with high reliability. These studies demonstrate algorithms' adaptability and effectiveness in tackling diverse optimization challenges, spanning energy systems, structural engineering, manufacturing, and agriculture. The findings collectively underscore the algorithm's potential to revolutionize problem-solving across scientific and industrial domains.

2.2 Rider Optimization Algorithm with Chaotic Maps Mechanisms (ROAC)

The Rider Optimization Algorithm is a metaheuristic technique inspired by the strategies of riders navigating challenging terrains. It categorizes riders into four roles to balance exploration and exploitation: bypass riders (leaders) guide the search, followers ensure steady progress, overtakers introduce diversity to avoid local optima, and attackers explore uncharted paths to enhance global search. These dynamic interactions enable the algorithm to adapt to complex optimization problems, making it effective for applications in engineering, resource allocation, and multi-objective decision-making. The methods described in this paper are intended to offer a comprehensive approach to optimization by addressing both theoretical and practical aspects. The solutions generated are not only optimal but also feasible and implementable in real-world scenarios as a result of the integration of sophisticated algorithms with domain-specific requirements. The subsequent sections provide a comprehensive examination of the specific integration strategies, the evaluation criteria, and the comparative performance analysis of the ROAC. It emulates the actions of riders, including the initial solution ($X_t(i,j)$) (**Equation (1)**), bypass riders ($X^B_{t+1}(i,j)$), followers ($X^F_{t+1}(i,k)$), overtakers($X^0_{t+1}(i,k)$), and attackers ($X^A_{t+1}(i,j)$), who employ a variety of strategies to reach their goal.

The ROAC is composed of four primary components: the bypass rider, follower, overtaker, and assailant. Each is essential in maintaining a balance between exploitation and exploration. Navigating the search space by combining the weighted coordinates of selected riders, the bypass rider functions as the leader, directing the population toward promising regions (**Equation (2)**). Followers closely model the circumvent rider's trajectory, thereby preserving diversity while refining convergence (**Equation (3)**). By incorporating both individual and leader positions, overtakers introduce dynamic search behaviors, enabling broader exploration to avoid local optima (**Equation (4)**). Attackers accelerate rapidly toward the leader,

guaranteeing rapid convergence (**Equation (5)**). In optimization problems that are constrained and unpredictable, these components function in a synergistic manner to ensure adaptability and robustness. Chaotic maps enhance ergodicity and allow the algorithm to effectively navigate complex landscapes.

$$X_t = \{X_t(i,j)\}, 1 \le i \le R, 1 \le j \le Q, 0 \le t \le T \quad (1)$$

$$X_{t+1}^{B}(i,j) = \delta\left[X_t(\eta,j)^{*}\beta(j) + X_t(\xi,j)^{*}[1-\beta(j)]\right] \quad (2)$$

$$X_{t+1}^{F}(i,k) = X^{L}(L,k) + \left|cos\left(T_{i,k}^{t}\right)^{*} X^{L}(L,k)^{*} d_i^t\right| \quad (3)$$

$$X_{t+1}^{0}(i,k) = X_t(i,k) + \lfloor D_t^I(i)^{*} X^{L}(L,k)\rfloor, where\ D_t^I(i) = \left\lfloor \frac{2}{1-\log\left(S_t^R(l)\right)} \right\rfloor - 1 \quad (4)$$

$$X_{t+1}^{A}(i,j) = X^{L}(L,j) + \left[cos\left(T_{i,j}^{t}\right) * X^{l}(L,j)\right] + d_i^t \quad (5)$$

The position updates for all riders are based on specific strategies: the bypass rider combines weighted positions of randomly selected riders, followers mimic the bypass rider's trajectory with adjustments guided by chaotic sequences, overtakers refine their movement by incorporating both self-information and the leader's position, and attackers accelerate toward the leader's position. The following provides a detailed explanation of the incorporation of chaotic maps into ROA's update rules in order to define their role in improving the algorithm's performance. The ROA incorporates chaotic maps by substituting the standard uniform random numbers used in the algorithm's position update rules with chaotic sequences generated by the selected maps (Logistic, Sinusoidal, and Iterative). The coordinates of the bypass rider, follower, overtaker, and assailant, as well as control parameters such as steering angle, gear, and acceleration coefficients, are initialized and updated by these sequences. This substitution incorporates deterministic but non-repetitive perturbations into the search process, thereby fostering ergodicity and diversity in the search space, thereby augmenting exploration and reducing the risk of premature convergence. This integration guarantees that the ROA maintains robustness in chaotic and constrained environments while maintaining a balanced exploration-exploitation trade-off.

The dynamic properties of chaotic maps and their documented efficacy in augmenting metaheuristic algorithms were carefully considered when selecting them for integration with the ROA. The Logistic, Sinusoidal, and Iterative maps were selected due to their unique ergodic characteristics and nonlinear behaviors, which enhance search diversity, prevent stagnation, and enhance robustness in chaotic and constrained environments. The algorithm is further improved by the incorporation of chaotic maps, which introduce dynamic, non-linear modifications to the search process, thereby improving exploration and exploitation. Chaotic sequences are generated by employing chaotic maps, including Logistic, Sinusoidal, and Iterative. These sequences are then used to initialize and update the motorcyclists' positions and control parameters. By investigating promising areas of the search space, the bypass rider (leader) in ROAC establishes a path for others. By closely imitating the bypass rider's trajectory, the followers ensure convergence toward the leader and update their positions. In order to achieve a balance between exploration and exploitation, overtakers integrate their information and the leader's position to refine their movement. Attackers accelerate the convergence process by approaching the leader's position at maximal speed. Parameters such as the steering angle, distance traveled, and weights are dynamically adjusted by the integration of chaotic maps, thereby facilitating a more robust search mechanism.

A boundary-handling mechanism is implemented to prevent constraint violations and guarantee that the solutions produced by the ROAC remain within the established boundaries. The following techniques are employed to correct a solution that exceeds the upper or lower limits: clamping, which ensures feasibility by restricting the value to the nearest boundary; and random reinitialization, which reassigns the solution within the valid range to maintain diversity in the search space. These strategies effectively prevent the algorithm from investigating infeasible regions and maintain a well-distributed population of solutions. The algorithm assures the stability of the optimization process, mitigates premature convergence caused by constraint violations, and enhances robustness by incorporating these boundary-handling methods. The ROAC parameters and their definitions are in **Table 1**. With 10 replicates, the ROAC parameters of [R, G, A, B, It] were set at [20, 5, Random[0,1], Random[0,1], 5000].

Table 1. ROA Parameters and Variables

Parameter or variable	Definition	Parameter or variable	Definition
t	Time instant	$X_t(i,k)$	Position of the i^{th} rider in the k^{th} coordinate
Q	Dimension of the optimization problem	$D_t^I(i)$	Route pointer of the i^{th} rider with the t prompt
X_t	Position of i^{th} rider at time t	$S_t^R(i)$	The i^{th} rider's success rate with the t instant time
δ	A random number within [0, 1]	$X^L(L,j)$	The leader's position
η	A random number within [1, R]	$T_{i,j}^t$	The steering angle of the i^{th} rider in the j^{th} coordinate
ξ	A random number that can be selected from 1 to R	R	Number of riders
β	A random number within [0, 1], but of size $1 \times Q$	S	Steering Angle
k	Coordinate selector	G	Gear
L	Index of bypass rider	A	Accelerator
X^L	Position of bypass rider	B	Brake
$T_{i,k}^t$	Steering angle in the k^{th} coordinate along with distance traveled by the i^{th} rider	It	Number of iterations
d_i^t	Distance to be traveled by the i^{th} rider		

Chaotic maps are frequently employed in optimization algorithms to generate well-distributed initial solutions, enhance search efficiency, and mitigate premature convergence by improving solution diversity. Unlike purely random initialization, chaotic sequences are deterministic yet non-repetitive, enabling comprehensive exploration of the search space. In this study, the chaotic sequences derived from the selected maps (Logistic, Sinusoidal, and Iterative) were first normalized to fit the predetermined boundaries of the decision variables. These normalized values were then projected onto the feasible solution space to ensure that the initial population remained both evenly distributed and diverse. By using chaotic maps during the early iterations, the global search capability of the algorithm is improved, thereby increasing the likelihood of identifying an optimal or near-optimal solution. This structured yet dynamic initialization process reduces the risk of getting trapped in local optima and improves the balance between exploration and exploitation. In particular, the Logistic map (**Equation (6)**) incorporates bifurcation behavior for controlled chaos, the Sinusoidal map (**Equation (7)**) provides seamless periodicity that is beneficial for convergence stability, and the Iterative map (**Equation (8)**) offers a higher level of complexity that is appropriate for robust search processes. The ROAC employs a structured process that capitalizes on the dynamic properties of chaos to optimize. The exploration and exploitation equilibrium during the search process are significantly enhanced by chaotic maps, where x_i is the current solution, x_{i+1} is the new solution, a = 0.5, it generates a chaotic sequence in (0, 1)

$$x_{i+1} = ax_i(1 - x_i) \tag{6}$$

$$x_{i+1} = ax_i^2\, sin(\pi x_i) \tag{7}$$

$$x_{i+1} = sin\left(\frac{a\pi}{x_i}\right) \tag{8}$$

Although other chaotic maps, including the Tent map **[22]** and Chebyshev map **[23]**, also demonstrate valuable dynamic features, this study prioritized a focused selection to ensure diversity in search dynamics and maintain experimental manageability. The ROAC consistently outperforms conventional methods across key metrics, including computational efficiency, solution accuracy, and constraint management, as confirmed by comparative analysis. Consequently, it is a potent instrument for addressing real-world optimization challenges. This foundation may be further developed in future research by assessing additional chaotic maps to improve the ROAC's performance across a variety of optimization problems. In real-world implementations, a chaotic system should ideally possess a large key space, exhibit complex dynamic behavior, and maintain an approximately uniform distribution

These maps introduce deterministic randomness, which allows the algorithm to circumvent local optima and obtain superior convergence. The positions of the motorcyclists within the defined search space

are initially initialized by a chaotic sequence generated by the selected chaotic map. The conventional ROA framework identifies four distinct strategic groups. Each of them follows different strategies aiming to accomplish its goals: A bypass rider attempts to approach the target point by avoiding the leader's trajectory to avoid direct competition. An overtaker aligns itself parallel to the leader by following it closely along a specified axis. The follower evaluates its present position by checking its nearby points to find a proper direction toward the goal. The attacker's goal is to try to force the leader to change his position by using maximum speed to reach its goal faster.

The utilization of chaotic maps in these revisions improves the exploration of the search space and increases the diversity of solutions. Boundary conditions are enforced following each update to guarantee that all passengers remain within the search space, and chaotic parameters are dynamically updated to facilitate exploration and exploitation. This iterative process persists until a stopping criterion is satisfied, such as convergence or a limit number of iterations. The algorithm's robustness is considerably enhanced by the integration of chaotic maps, which diversify the search trajectories and prevent premature convergence.

The algorithm ultimately returns the optimal solution and its corresponding fitness value, thereby illustrating the efficacy of integrating chaotic dynamics with ROAC to address intricate optimization problems. The pseudocode illustrating the ROAC and its key parameters is presented below.

Begin;
Initialize positions using a chaotic sequence and define algorithm parameters
steering angle: S, gear: G, accelerator: A,
Brake: B and maximum time: T_{off}
For i = 1 to Max replication;
For j = 1 to Max Iteration;
Initialise and rank the initial solution R (No. of riders)
Evaluate the fitness values of all riders and partition them into four groups
Calculate the success rate
Update positions for all riders:
- Bypass rider: Weighted combination of random positions.
- Follower: Mimics leader with chaotic adjustments.
- Overtaker: Combines self and leader positions.
- Attacker: Moves directly toward the leader.
Rider's positions are arranged based on the success rate
The rider showing the highest success rate is referred to as the leading rider.
Update the rider's parameters
Enforce boundaries and update chaotic parameters.
End for;
End for;
End;
End procedure;

3. RESULTS AND DISCUSSION

Three chaotic maps (Logistic, Sinusoidal, and Iterative) were added to the Rider Optimization Algorithm to address two classes of optimization problems. The first class includes eight noisy response surface benchmarks—Branin (**Equation (9)**), Camelback (**Equation (10)**), Goldstein-Price (**Equation (11)**), Parabolic (**Equation (12)**), Rastrigin (**Equation (13)**), Rosenbrock (**Equation (14)**), Shekel (**Equation (15)**), and Styblinski (**Equation (16)**)—selected for their complicated landscapes, including non-convexity, multimodality, and irregular structures where x_i denotes the dimension of the optimization problem, a_j and a_{ij} denote the constant of the optimization problem.

These benchmarks assessed the algorithm's performance in noisy and difficult terrain. The noise is normally distributed with a mean of 0 and standard deviations of 0.5 and 1.

$$f(x) = -5\log_{10}\left[\left(x_2 - \frac{5.1}{4\pi^2}x_1^2 + \frac{5}{\pi}x_1 - 6\right)^2 + \left(10 - \frac{5}{4\pi}\cos(x_1)\right) + 10\right] \tag{9}$$

$$f(x) = 10 - \log_{10}\left[x_1^2\left(4 - 2.1x_1^2 + \frac{1}{3}x_1^4\right) + x_1x_2 + 4x_2^2(x_2^2 + 1)\right] \tag{10}$$

$$f(x) = 10 + \log_{10}\left[\begin{array}{c}\dfrac{1}{\{1 + (1 + x_1 + x_2)^2(19 - 14x_1 + 3x_1^2 - 14x_2 + 6x_1x_2 + 3x_2^2)\}} \\ * \{30 + (2x_1 - 3x_2)^2(18 - 32x_1 + 12x_1^2 + 48x_2 - 36x_1x_2 + 27x_2^2)\}\end{array}\right] \tag{11}$$

$$f(x) = 12 - \sum_{j=1}^{k}\left[\frac{(-x_j)^2}{100}\right] \tag{12}$$

$$f(x) = 80 - \left[20 + \sum_{i=1}^{n} x_i^2 - 10\left(\sum_{i=1}^{n} \cos 2\pi x_i\right)\right] \tag{13}$$

$$f(x) = 70\left[\frac{\left(\left\{20 - \left(\left(-\frac{x_1}{a_1}\right)^2 + \sum_{j=2}^{k}\left[\left(\frac{x_j}{a_j}\right) - \left(\frac{x_1}{a_1}\right)^2\right]^2\right)\right\} + 150\right)}{170}\right] + 10 \tag{14}$$

$$f(x) = 100\sum_{i=1}^{n} \frac{1}{c_i + \sum_{j=1}^{k}(x_j - a_{ij})^2} \tag{15}$$

$$f(x) = 275 - \left[\left(\frac{(x_1^4 - 16x_1^2 + 5x_1)}{2}\right) + \left(\frac{(x_2^4 - 16x_2^2 + 5x_2)}{2}\right) + \sum_{i=3}^{5}(x_i - 1)^2\right] \tag{16}$$

The second class includes two multi-objective optimization problems: the first model is to optimize machining parameters like cutting speed (T_P), feed rate (C_P), and depth of cut (R_a) while meeting equipment and safety constraints (**Equation (17)**) **[24]**, and the second is to design a multiple-disk clutch brake system to minimize material volume ($f_1(\vec{z})$) and torque ($f_2(\vec{z})$) under strict engineering and dimensional constraints (**Equation (18)**) **[25]**.

$$\begin{gathered} Min\ T_P = 0.12 + 231376(1 + 0.26/T)MRR + 0.04 \\ Min\ C_P = (13.55/T + 0.39)T_P \\ Min\ R_a = 0.0088v + 0.3232f + 0.3144a \end{gathered} \tag{17}$$

Subject to:

$$\begin{gathered} T = 1575134.21(v^{-1.7}f^{-1.55}a^{-1.22}) \\ MRR = 1000vfa \\ 70 \le v \le 90 \\ 0.1 \le f \le 2 \\ 0.1 \le a \le 5 \\ 0.000626(vf^{1.18}a^{1.26}) \le 5 \\ 1.38(f^{1.18}a^{1.26}) \le 230 \end{gathered}$$

$$\begin{gathered} Minimize\ f_1(\vec{z}) = M = \pi(r_0^2 - r_i^2)t(Z+1)p_m \\ Minimize\ f_2(\vec{z}) = T = \frac{I_z w}{M_h + M_f} \end{gathered} \tag{18}$$

Subject to:

$$\begin{gathered} g_1(\vec{z}) = r_0 - r_i - \Delta R \ge 0 \\ g_2(\vec{z}) = L_{max} - (Z+1)(t+\delta) \ge 0, \\ g_3(\vec{z}) = p_{max} - p_{rz} \ge 0, \\ g_4(\vec{z}) = p_{xax}V_{sr,max} - p_{rz}V_{sr} \ge 0, \\ g_5(\vec{z}) = V_{sr,max} - V_{sr} \ge 0, \\ g_6(\vec{z}) = M_h - sM_s \ge 0, \\ g_7(\vec{z}) = T \ge 0, \\ g_8(\vec{z}) = T_{max} - T \ge 0, \\ 60 \le r_i \le 80\ mm, \\ 90 \le r_0 \le 100\ mm, \\ 1.5 \le T \le 3\ mm, \\ 0 \le F \le 1000\ N, \\ 2 \le Z \le 9 \end{gathered}$$

The ROAC framework enhances both exploration and exploitation, accelerating convergence and improving solution quality in high-dimensional and constrained optimization problems. The notations and abbreviations employed in the multi-objective machining optimization problem ensure that all symbols and parameters are explicitly defined in **Table 2**. Parameter settings are followed: ΔR = 20 mm, L_{max} = 30 mm, $V_{sr,max}$ = 10 m/s, μ = 0.5, δ = 0.5 mm, M_s = 40 Nm, M_f = 3 Nm, n = 250 rpm, p_{max} = 1 MPa, I_z = 55 kg.m^2, T_{max} = 15s, and ρ = 7800 kg/m3, $r_i \in$ (60, 61, 62,…, 80), $r_0 \in$ (90, 91,…,110), $t \in$ (1, 1.5, 2, 2.5, 3), $F \in$ (600, 610, 620,…,1000) and $Z \in$ (2, 3, 4, 5, 6, 7, 8, 9).

Table 2. Notations and Abbreviations Used in the Multi-Objective Machining Optimization Problem

Parameters	Definition	Parameters	Definition
T_p	Unit machining time (min)	C_t	Tool cost ($)
π	Mathematical constant (3.1415)	C_I	Labor cost ($/min)
C_p	Unit machining cost per product ($)	C_o	Overhead cost ($/min)
R_a	Roughness of the finished surface (μm)	$K_F, K_n, k, x_1, x_2, x_3$	Constants relevant to a specific tool–work piece
MRR	Material removal rate (mm^3/min)	$K_T, \alpha_1, \alpha_2, \alpha_3, \beta_1, \beta_2, \beta_3$	Positive constant parameters
T_s	Tool setup time (min)	V	Volume of the removed metal (mm^3)
T_c	Tool change time (min)	η	Mechanical efficiency of the machine (%)
T_i	Tool non-cutting time (min)	v_{min}, v_{max}	Boundary of cutting speed (m/min)
f_{min}, f_{max}	Boundary of feed rate (mm/rev)	F_{max}, P_{max}	Maximum cutting force (N) and cutting power (kw)
a_{min}, a_{max}	Boundary of depth of cut (mm)		

The ROAC was selected for its ability to tackle complex optimization problems involving noisy response surfaces and constrained search spaces. Traditional algorithms often struggle with premature convergence and local optima entrapment, while ROA maintains a strong balance between exploration and exploitation for adaptive search [26]-[28]. However, its standard version may underperform in irregular landscapes and is sensitive to initial conditions. To enhance performance, Logistic, Sinusoidal, and Iterative chaotic maps were integrated into the standard ROA [29], leveraging their ergodicity and randomness to improve search diversity, accelerate convergence, and enhance robustness. Benchmark tests and real-world applications confirmed that chaotic ROA outperformed the conventional variant in convergence speed, accuracy, stability, and constraint management. Lower standard deviations indicated greater solution stability in noisy environments. Multi-objective tasks, such as clutch brake optimization, validated its effectiveness in maintaining feasibility without compromising optimality. The comparative analysis further demonstrated that chaotic maps significantly enhance metaheuristic algorithms, establishing ROAC as a powerful tool for solving complex real-world optimization challenges.

3.1 Response Surface Benchmarks

The ROAC increased resilience, precision, and adaptability across both problem domains by using chaotic maps' dynamic, nonlinear features. This paper examines the algorithm's performance to see how well this hybrid technique handles noisy response surfaces and complex multi-objective optimization problems (Figure 1). The ROAC and its chaotic map-enhanced variants—Logistic (ROAC1), Sinusoidal (ROAC2), and Iterative (ROAC3)—are demonstrated to be effective in optimizing eight benchmark response surfaces under varying noise levels (0, 0.5, and 1.0) in the experiments. The effectiveness and stability of various optimization methods are contingent upon the function in a noise-free environment. ROAC3 consistently produces the most consistent results, exhibiting the lowest standard deviation across the majority of functions. In the Branin function, ROA exhibits minimal variability and near-optimal results. In the meantime, ROAC1 maintains resilient stability and excels in the Goldstein-Price and Shekel functions. ROAC3 guarantees superior consistency and near-optimal values for the Rastrigin and Styblinski functions (Figure 2), which are extremely sensitive. Parabolic and Rosenbrock functions are undisturbed by any method, exhibiting no variation. In general, ROAC3 is the preferred procedure in noise-free conditions because of its high robustness and negligible variance.

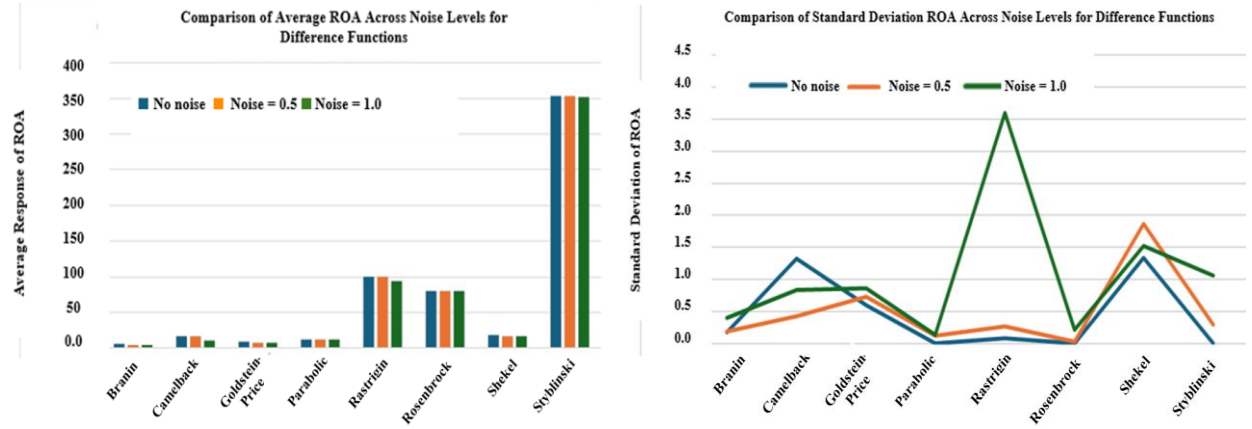

Figure 1. Comparison of the Mean and Standard Deviation of ROA Across Different Noise Levels for Each Function

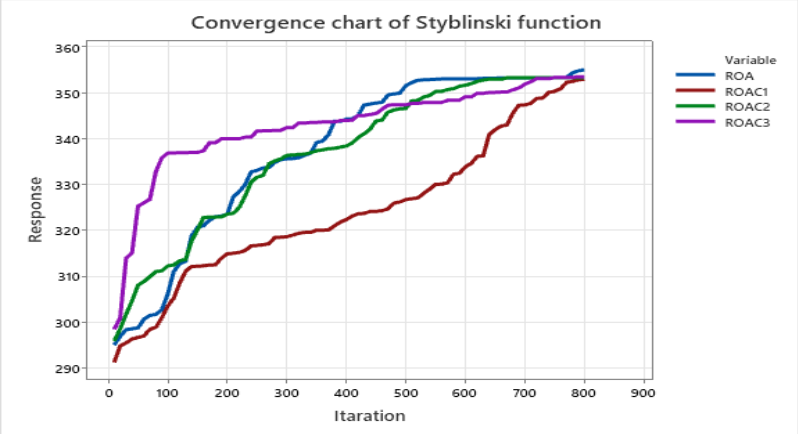

Figure 2. Convergence of the Algorithms When the Response Is Noise-Free

At a moderate noise level of 0.5, different methods adapt with varying effectiveness, causing slight performance shifts. ROAC3 remains highly resilient in the Rastrigin and Styblinski functions, while ROAC1 excels in Camelback and Shekel functions due to its superior handling of fluctuations. ROAC2 shows the highest variance and lowest average response in the Goldstein-Price function, making it more noise-sensitive, whereas ROA demonstrates strong noise resistance in the Branin function. Parabolic and Rosenbrock functions remain stable across all methods. Overall, ROAC3 ensures the best stability, but ROAC1 is preferable for noise-sensitive functions. At a higher noise level of 1.0, method distinctions become more pronounced. ROAC1 is the most stable across Branin, Camelback, and Shekel functions, maintaining low variance. ROAC3 continues to perform well in Rastrigin, showcasing its ability to navigate complex search spaces. ROAC2 delivers reliable average responses in Goldstein-Price but suffers from high standard deviation, making it less dependable in fluctuating conditions.

Standard ROA struggles in Camelback and Goldstein-Price, proving unsuitable for high-noise environments. Parabolic and Rosenbrock functions remain stable across all methods. ROAC3 is the most effective in noise-free conditions, while ROAC1 provides the most consistent performance at higher noise levels, making it the best choice for managing extreme noise scenarios. In terms of overall performance, stability, and resilience to noise fluctuations, ROAC3 is the most effective optimization method when taking into account all noise levels and function responses. Although ROAC1 exhibits significant adaptability in high-noise environments, ROAC3 maintains its dominance across a broader spectrum of functions. ROAC3 is the optimal choice for optimization tasks across a variety of function types and noise levels due to its capacity to consistently produce optimal results with minimal variance (Figure 3).

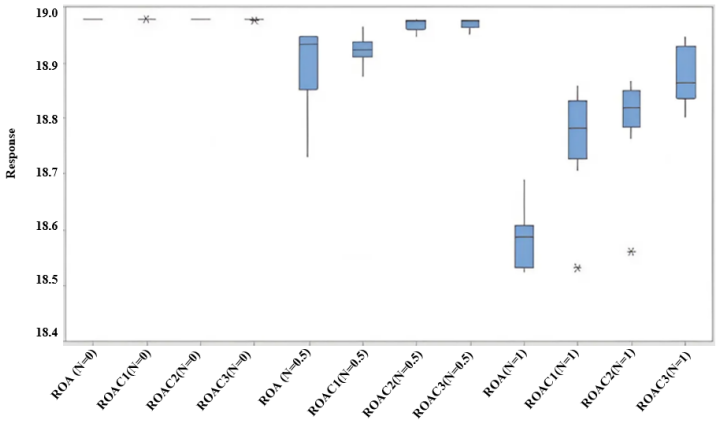

Figure 3. Central Tendency and Dispersion Effect for all Levels of Shekel Function

The ROAC variants demonstrated their robustness under moderate noise (0.5), with ROAC1 and ROAC2 achieving higher Branin function averages (5.0702 and 4.9764) than ROA (4.8451), while ROAC1 also minimized standard deviation (0.1951). ROAC3 excelled in the Camelback function with the highest average (17.3029) and competitive stability (stdev 0.7577). In chaotic multimodal functions like Rastrigin, ROAC2 and ROAC3 maintained superior consistency with low standard deviations (0.0051 and 0.0153), ensuring reliable performance in uncertain conditions. At higher noise levels (1.0), chaotic maps further improved performance. ROAC3 achieved the highest average fitness in Branin (4.8893) with balanced stability (stdev 0.3321), while ROAC2 maintained accuracy and stability in complex landscapes like Shekel (stdev 0.11). Despite increased uncertainty, chaotic maps enhanced ROA's ability to explore and exploit effectively, leading to superior outcomes when compared to Data Envelopment Analysis-based Ranking (DEAR) **[30]**. The experimental results confirm the adaptability of the standard ROA and its chaotic variants (ROAC1, ROAC2, ROAC3), achieving an optimal balance between exploration and exploitation. With parameters set at R = 20, G = 5, iterations = 5000, and replications = 15, the chaotic-enhanced ROA consistently converged to global optima in constrained and multi-variable scenarios.

3.2 Multi-Objective Optimization Problems

ROAC and its chaotic variants exhibited robust performance in the multiple disk clutch brake design problem, demonstrating their effectiveness in constrained engineering optimization. ROAC3 achieved the global minimum objective value (0.2352), performing on par with benchmark algorithms such as Transient Search Algorithm (TSO), Moth-Flame Optimization (MFO), Whale Optimization Algorithm (WOA), Coot Optimization Algorithm (COOT), Multi-Verse Optimization (MVO), Arithmetic Optimization Algorithm (AOA), Sine Cosine Algorithm (SCA), Seagull Optimization Algorithm (SOA), and Pelican Optimization Algorithm (POA). The numerical results were obtained from previous literature **[31]** and validated through multiple independent runs to ensure consistency. ROA and its chaotic variants were programmed using Visual Studio 2022, leveraging built-in numerical optimization libraries to efficiently handle complex search spaces and computational constraints. The integration of chaotic maps improved the algorithm's adaptability and enhanced its ability to navigate high-dimensional constrained landscapes, further reinforcing its suitability for real-world engineering applications. The algorithm's stability and reliability were considerably improved by the chaotic maps, as demonstrated by the minimal deviation in design parameters across ROAC1, ROAC2, and ROAC3. Although ROAC1 and ROAC2 generated objective values that were marginally higher (0.2356 and 0.2354, respectively), their performance was competitive, thereby validating the ability of chaotic enhancements to manage complex constraints (**Table 3**).

Table 3. Comparison of the Best Optimal Solutions of Multiple Disks Clutch Brake Design Problem

Algorithm	X_1	X_2	X_3	X_4	X_5	Min
TSO	70.00	90.00	1.00	871.24	2.00	0.235
MFO	70.00	90.00	1.00	958.62	2.00	0.235
WOA	70.00	90.00	1.00	1000.00	2.00	0.235
COOT	70.00	90.00	1.00	859.81	2.00	0.235
MVO	69.99	90.00	1.00	999.83	2.00	0.235
AOA	70.01	90.04	1.00	1000.00	2.00	0.235

Algorithm	X_1	X_2	X_3	X_4	X_5	Min
SCA	69.99	90.00	1.00	1000.00	2.00	0.235
SOA	70.00	90.00	1.00	965.93	2.00	0.235
POA	62.32	94.44	2.77	659.55	4.39	0.235
ROA	69.94	89.99	1.00	966.88	2.00	0.236
ROAC1	69.55	89.67	1.00	971.13	2.00	0.236
ROAC2	69.17	89.36	1.00	962.56	2.00	0.235
ROAC3	69.77	89.82	1.00	964.33	2.00	0.235

In particular, ROAC3 demonstrated exceptional convergence reliability by effectively balancing early-stage exploration and late-stage exploitation (**Figure 4**). In problems with limited feasible regions, this hybrid dynamic is particularly advantageous, as the chaotic maps diversify the search process, thereby preventing premature convergence. The efficacy of ROAC3 as a dependable instrument for constrained design optimization is further substantiated by its comparable performance to top-tier algorithms.

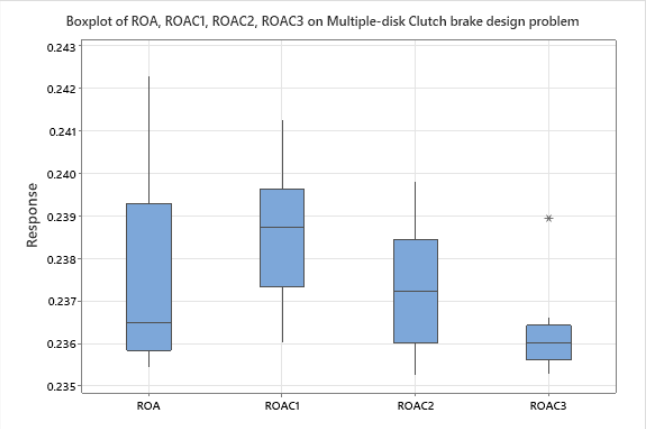

Figure 4. Performance Measures of ROA and Its Variants on the Response

The ROAC variants in the multi-pass turning problem successfully balanced a variety of conflicting objectives, such as machining time, cost, surface imperfection, material removal rate (MRR), and energy consumption. Although the Hybrid Self-Adaptive Firefly Algorithm (HSFLA3) and base ROA obtained higher cutting speeds and MRR, the chaotic-enhanced variants provided a more comprehensive trade-off. ROAC1, ROAC2, and ROAC3 consistently achieved competitive MRR while preserving superior surface finish and reduced energy consumption, rendering them highly suitable for scenarios that necessitate multi-objective optimization **[31]**. The consistent clustering of objective function values (Z = 0.8186) across ROAC1, ROAC2, and ROAC3 was indicative of the robustness of chaotic maps. Additionally, these variants exhibited decreased variability in machining parameters while maintaining a balance between quality, cost efficiency, and productivity (**Table 4**). This balanced approach emphasizes the potential of chaotic ROA variants in practical manufacturing applications, where precision and efficiency must coexist.

Table 4. Comparison of the Best Optimal Solutions of the Multi-Pass Turning Problem

Parameter	ROA	ROAC1	ROAC2	ROAC3
$v\ (mm/min)$	99.692	99.177	98.930	99.226
$f\ (mm/rev)$	1.9921	1.9807	1.9860	1.9943
$a\ (mm)$	4.9850	4.9970	5.0000	4.9984
$T_P\ (min)$	0.3957	0.3977	0.3975	0.3959
$C_P\ (\$)$	0.3300	0.3291	0.3291	0.3297
$R_a\ (\mu m)$	3.0884	3.0840	3.0845	3.0892
$MRR\ (mm^3/min)$	990004.68	981626.56	982394.49	989121.14
$T\ (min)$	30.5148	30.9680	30.9481	30.6055
$F\ (N)$	23.5574	23.4696	23.5616	23.6679
$P\ (kw)$	0.0879	0.0873	0.0872	0.0875
Z	0.8186	0.8186	0.8186	0.8186

The incorporation of chaotic maps into the standard ROA significantly improved its adaptability, reliability, and robustness in both optimization problems. For instance, ROAC3 obtained the highest objective value of 0.2352 in the multiple disk clutch brake design problem, which was equivalent to or greater than benchmark algorithms such as TSO, MFO, and WOA [28]. The chaotic ROA variants consistently exhibited superior stability, as evidenced by their lower standard deviations across noisy response surface benchmarks, such as 0.3321 in the Branin function at noise level 1.0. In the same benchmark, ROAC1 and ROAC2 delivered competitive performance, with best objective values of 0.236, while ROAC3 consistently demonstrated superior precision and convergence reliability. The algorithm's efficiency was underscored by the ROA's comparable performance to its chaotic variants in simpler optimization landscapes, such as the Rosenbrock and Parabolic functions [31]. Nevertheless, the ROAC variants considerably enhanced the algorithm's ability to balance exploration and exploitation, resulting in superior results in complex and multimodal functions such as Rastrigin and Camelback. These quantitative results underscore the practical value of ROAC1, ROAC2, and ROAC3 as adaptable instruments for real-world engineering problems that necessitate the simultaneous optimization of conflicting objectives and constraints.

4. CONCLUSION

The increasing complexity of optimization problems involving chaotic response surfaces and constrained functions has driven interest in enhancing metaheuristic techniques. This study improves the standard Rider Optimization Algorithm (ROA) by integrating chaotic maps or ROAC, leveraging their stochastic and ergodic properties to enhance constraint management, prevent premature convergence, and navigate complex landscapes. Experimental results confirm that the ROAC variants consistently outperform its conventional counterpart by balancing exploration and exploitation, improving accuracy, and accelerating convergence. For instance, in the multiple disk clutch brake design problem, the algorithm achieved the best objective value of 0.2352, matching or surpassing benchmark algorithms such as TSO, MFO, and WOA. Additionally, in noisy response surface benchmarks, the ROAC achieved lower standard deviations (e.g., 0.3321 in the Branin function at noise level 1.0), demonstrating superior stability and robustness. Integrated constraint-handling mechanisms ensured feasible solutions without sacrificing optimality, further highlighting the potential of chaotic maps in advancing metaheuristic optimization.

In practice, the ROAC variants demonstrate exceptional adaptability and dependability in the face of scheduling, resource allocation, and engineering design challenges. It is notably advantageous for real-world applications in manufacturing, where it optimizes machining processes, reduces costs, and increases productivity, due to its capacity to manage constraints and uncertainties. In the renewable energy sector, it effectively allocates resources for wind and solar systems, optimizing output and cost, while the aerospace and automotive industries benefit from its precision in designing intricate components. These discoveries provide a basis for optimization algorithms that are specific to the requirements of a particular industry. In addition to manufacturing and energy, the ROAC variants can enhance the efficacy of medical imaging, optimize hospital scheduling, and expedite supply chain operations by optimizing routing and inventory management in constrained environments. It is an effective instrument for complex decision-making due to its capacity to manage multiple conflicting objectives. Future research should concentrate on the scalability of the ROAC variants for large-scale optimization problems, the hybridization of other chaotic maps, such as Tent and Chebyshev, with other metaheuristic techniques, and the exploration of broader applications in artificial intelligence, renewable energy, and healthcare. Ultimately, this study underscores the transformative potential of the ROAC variants in addressing real-world optimization challenges, fostering innovation, and enhancing operational efficiency across a variety of industries.

AUTHOR CONTRIBUTIONS

Pongchanun Luangpaiboon: Conceptualization, Data Curation, Formal Analysis, Funding Acquisition, Investigation, Methodology, Resources, Supervision, Validation, Writing - Original Draft, Writing - Review and Editing. Danupun Visuwan: Data Curation, Funding Acquisition, Writing - Original Draft, Writing - Review and Editing. Atiwat Nanphang: Funding Acquisition, Visualization, Writing - Original Draft, Writing - Review and Editing. Lakkana Ruekkasaem: Funding Acquisition, Project Administration, Writing - Original Draft, Writing - Review and Editing. Pasura Aungkulanon: Conceptualization, Data Curation, Formal

analysis, Funding Acquisition, Investigation, Methodology, Resources, Software, Validation, Writing - Original Draft, Writing - Review and Editing. All authors discussed the results and contributed to the final manuscript.

FUNDING STATEMENT

This research has been funded by the Faculty of Engineering, Thammasat School of Engineering, Thammasat University: Contract No. 001/2568.

ACKNOWLEDGMENT

Our Gratitude to the Faculty of Engineering, King Mongkut's University of Technology North Bangkok, for supporting this research.

CONFLICT OF INTEREST

The authors declare no conflicts of interest to report study.

REFERENCES

[1] A. K. T and E. J. T. Fredrik, "SEGMENTING AND IDENTIFYING SPINAL TUBERCULOSIS DISEASE USING AN ENHANCED CSA AND RIDER OPTIMIZATION TECHNIQUE," *International Journal of Intelligent Systems and Applications in Engineering*, vol. 12, no. 16s, pp. 562 - 570, 02/23 2024. [Online]. Available: https://www.ijisae.org/index.php/IJISAE/article/view/4893.

[2] K. Mehmood, N. I. Chaudhary, Z. A. Khan, K. M. Cheema, and M. A. Zahoor Raja, "ATOMIC PHYSICS-INSPIRED ATOM SEARCH OPTIMIZATION HEURISTICS INTEGRATED WITH CHAOTIC MAPS FOR IDENTIFICATION OF ELECTRO-HYDRAULIC ACTUATOR SYSTEMS," *Modern Physics Letters B*, vol. 38, no. 30, p. 2450308, 2024/10/30 2024, doi: https://doi.org/10.1142/S0217984924503081.

[3] O. N. Roeva and D. Zoteva, "A COMPARISON OF CHAOTIC ELECTROMAGNETIC FIELD OPTIMIZATION ALGORITHMS," *International Journal Bioautomation*, vol. 28, no. 4, pp. 245–265, Dec.2024, doi: https://doi.org/10.7546/ijba.2024.28.4.000970.

[4] S. N. Roopa, P. Anandababu, S. Amaran, and R. Verma, "METAHEURISTIC SECURE CLUSTERING SCHEME FOR ENERGY HARVESTING WIRELESS SENSOR NETWORKS," *Computer Systems Science and Engineering*, vol. 45, no. 1, 2023, doi: https://doi.org/10.32604/csse.2023.029133.

[5] S. Kumbhare, A. B.Kathole, and S. Shinde, "FEDERATED LEARNING AIDED BREAST CANCER DETECTION WITH INTELLIGENT HEURISTIC-BASED DEEP LEARNING FRAMEWORK," *Biomedical Signal Processing and Control*, vol. 86, p. 105080, 2023/09/01/ 2023, doi: https://doi.org/10.1016/j.bspc.2023.105080.

[6] S. K. Sarangi, A. Nanda, R. Lenka, and P. K. Behera, "HYBRID HEURISTIC DRIVING TRAINING-RIDER OPTIMIZATION ALGORITHM FOR QOS-AWARE MULTICAST COMMUNICATION SYSTEM IN MANET," *Australian Journal of Electrical and Electronics Engineering*, vol. 21, no. 1, pp. 59-78, 2024/01/02 2024, doi: https://doi.org/10.1080/1448837X.2024.2309428.

[7] D. K. A and R. J, "ENERGY EFFICIENT CLUSTERING AND ROUTING USING HYBRID FUZZY WITH MODIFIED RIDER OPTIMIZATION ALGORITHM IN IOT - ENABLED WIRELESS BODY AREA NETWORK," *Journal of Machine and Computing*, vol. 3, no. 2, pp. 171–183, Apr. 2023, doi: https://doi.org/10.53759/7669/jmc202303016.

[8] M. Alazab, K. Lakshmanna, T. R. G, Q.-V. Pham, and P. K. Reddy Maddikunta, "MULTI-OBJECTIVE CLUSTER HEAD SELECTION USING FITNESS AVERAGED RIDER OPTIMIZATION ALGORITHM FOR IOT NETWORKS IN SMART CITIES," *Sustainable Energy Technologies and Assessments*, vol. 43, p. 100973, 2021/02/01/ 2021, doi: https://doi.org/10.1016/j.seta.2020.100973.

[9] R. K. Prasad and T. Jaya, "INTELLIGENT SPECTRUM SHARING AND SENSING IN COGNITIVE RADIO NETWORK BY USING AROA (ADAPTIVE RIDER OPTIMIZATION ALGORITHM)," *International Journal of Computational Intelligence and Applications*, vol. 22, no. 01, p. 2341007, 2023, doi: https://doi.org/10.1142/S1469026823410079.

[10] M. S. Deelip and K. Govinda, "EXPSFROA-BASED DRN: EXPONENTIAL SUNFLOWER RIDER OPTIMIZATION ALGORITHM-DRIVEN DEEP RESIDUAL NETWORK FOR THE INTRUSION DETECTION IN IOT-BASED PLANT DISEASE MONITORING," *International Journal of Semantic Computing*, vol. 17, no. 01, pp. 5-31, 2023, doi: https://doi.org/10.1142/S1793351X22400165.

[11] N. K. Raja, E. L. Lydia, T. A. Acharya, K. Radhika, E. Yang, and O. Yi, "RIDER OPTIMIZATION WITH DEEP LEARNING BASED IMAGE ENCRYPTION FOR SECURE DRONE COMMUNICATION," *IEEE Access*, vol. 11, pp. 121646-121655, 2023, doi: https://doi.org/10.1109/ACCESS.2023.3324068.

[12] J. Xu and B. Li, "UNCERTAIN UTILITY PORTFOLIO OPTIMIZATION BASED ON TWO DIFFERENT CRITERIA AND IMPROVED WHALE OPTIMIZATION ALGORITHM," *Expert Systems with Applications*, vol. 268, p. 126281, 2025/04/05/ 2025, doi: https://doi.org/10.1016/j.eswa.2024.126281 .

[13] S. Benghazouani, S. Nouh, and A. Zakrani, "OPTIMIZING BREAST CANCER DIAGNOSIS: HARNESSING THE POWER OF NATURE-INSPIRED METAHEURISTICS FOR FEATURE SELECTION WITH SOFT VOTING CLASSIFIERS," *International Journal of Cognitive Computing in Engineering*, vol. 6, pp. 1-20, 2025/12/01/ 2025, doi: https://doi.org/10.1016/j.ijcce.2024.09.005.

[14] Z. Chen, S. Li, A. T. Khan, and S. Mirjalili, "COMPETITION OF TRIBES AND COOPERATION OF MEMBERS ALGORITHM: AN EVOLUTIONARY COMPUTATION APPROACH FOR MODEL FREE OPTIMIZATION," *Expert Systems with Applications*, vol. 265, p. 125908, 2025/03/15/ 2025, doi: https://doi.org/10.1016/j.eswa.2024.125908.

[15] M. Alibeigi, R. Jazmi, R. Maddahian, and H. Khaleghi, "INTEGRATED STUDY OF PREDICTION AND OPTIMIZATION PERFORMANCE OF PBI-HTPEM FUEL CELL USING DEEP LEARNING, MACHINE LEARNING AND STATISTICAL CORRELATION," *Renewable Energy*, vol. 235, p. 121295, 2024/11/01/ 2024, doi: https://doi.org/10.1016/j.renene.2024.121295.

[16] T. Palaniappan and P. Subramaniam, "INVESTIGATION IN OPTIMIZATION OF PROCESS PARAMETERS IN TURNING OF MILD STEEL USING RESPONSE SURFACE METHODOLOGY AND MODIFIED DEEP NEURAL NETWORK," *Materials Today Communications*, vol. 38, p. 108425, 2024/03/01/ 2024, doi: https://doi.org/10.1016/j.mtcomm.2024.108425.

[17] D. Rajamani, M. Siva Kumar, and E. Balasubramanian, "CHAPTER 27 - MULTI-RESPONSE OPTIMIZATION OF PLASMA ARC CUTTING ON MONEL 400 ALLOY THROUGH WHALE OPTIMIZATION ALGORITHM," in *Handbook of Whale Optimization Algorithm*, S. Mirjalili Ed.: Academic Press, 2024, pp. 373-386. doi: 10.1016/B978-0-32-395365-8.00033-6.

[18] K. Kalita, R. K. Ghadai, and S. Chakraborty, "A COMPARATIVE STUDY ON MULTI-OBJECTIVE PARETO OPTIMIZATION OF WEDM PROCESS USING NATURE-INSPIRED METAHEURISTIC ALGORITHMS," *International Journal on Interactive Design and Manufacturing (IJIDeM)*, vol. 17, no. 2, pp. 499-516, 2023/04/01 2023, doi: 10.1007/s12008-022-01007-8.

[19] E. Kawecka, "THE WHALE OPTIMIZATION ALGORITHM IN ABRASIVE WATER JET MACHINING OF TOOL STEEL," *Procedia Computer Science*, vol. 225, pp. 1037-1044, 2023/01/01/ 2023, doi: https://doi.org/10.1016/j.procs.2023.10.091.

[20] P. Kumar, P. Gupta, and I. Singh, "PARAMETRIC OPTIMIZATION OF FDM USING THE ANN-BASED WHALE OPTIMIZATION ALGORITHM," *Artificial Intelligence for Engineering Design, Analysis and Manufacturing*, vol. 36, p. e27, 2022, Art no. e27, doi: 10.1017/S0890060422000142.

[21] Z. Liu, L. Zhang, J. Li, and M. Mamluki, "PREDICTING THE SEISMIC RESPONSE OF THE SHORT STRUCTURES BY CONSIDERING THE WHALE OPTIMIZATION ALGORITHM," *Energy Reports*, vol. 7, pp. 4071-4084, 2021/11/01/ 2021, doi: https://doi.org/10.1016/j.egyr.2021.06.095.

[22] Y. Qi, A. Jiang, and Y. Gao, "A GAUSSIAN CONVOLUTIONAL OPTIMIZATION ALGORITHM WITH TENT CHAOTIC MAPPING," *Scientific Reports*, vol. 14, no. 1, p. 31027, 2024, doi: 10.1038/s41598-024-82277-y.

[23] I. Gagnon, A. April, and A. Abran, "AN INVESTIGATION OF THE EFFECTS OF CHAOTIC MAPS ON THE PERFORMANCE OF METAHEURISTICS," *Engineering Reports*, vol. 3, no. 6, p. e12369, 2021, doi: 10.1002/eng2.12369.

[24] P. Aungkulanon and P. Luangpaiboon, "VERTICAL TRANSPORTATION SYSTEMS EMBEDDED ON SHUFFLED FROG LEAPING ALGORITHM FOR MANUFACTURING OPTIMISATION PROBLEMS IN INDUSTRIES," *SpringerPlus*, vol. 5, no. 1, p. 831, 2016/06/22 2016, doi: 10.1186/s40064-016-2449-1.

[25] G. Dhiman and V. Kumar, "MULTI-OBJECTIVE SPOTTED HYENA OPTIMIZER: A MULTI-OBJECTIVE OPTIMIZATION ALGORITHM FOR ENGINEERING PROBLEMS," *Knowledge-Based Systems*, vol. 150, pp. 175-197, 2018/06/15/ 2018, doi: https://doi.org/10.1016/j.knosys.2018.03.011.

[26] Y. Fu, Z. Li, N. Chen, and C. Qu, "A DISCRETE MULTI-OBJECTIVE RIDER OPTIMIZATION ALGORITHM FOR HYBRID FLOWSHOP SCHEDULING PROBLEM CONSIDERING MAKESPAN, NOISE AND DUST POLLUTION," *IEEE Access*, vol. 8, pp. 88527-88546, 2020, doi: 10.1109/ACCESS.2020.2993084.

[27] Kumar Rahul, Rohitash Kumar, and Banyal, "RIDER OPTIMIZATION ALGORITHM (ROA): AN OPTIMIZATION SOLUTION FOR ENGINEERING PROBLEM," *Turkish Journal of Computer and Mathematics Education*, vol. 12, no. 12, pp. 3197–3201, 2021, doi: https://doi.org/10.17762/turcomat.v12i12.7994.

[28] G. Wang, Y. Yuan, and W. Guo, "AN IMPROVED RIDER OPTIMIZATION ALGORITHM FOR SOLVING ENGINEERING OPTIMIZATION PROBLEMS," *IEEE Access*, vol. 7, pp. 80570-80576, 2019, doi: 10.1109/ACCESS.2019.2923468.

[29] R. B. Naik and U. Singh, "A REVIEW ON APPLICATIONS OF CHAOTIC MAPS IN PSEUDO-RANDOM NUMBER GENERATORS AND ENCRYPTION," *Annals of Data Science*, vol. 11, no. 1, pp. 25-50, 2024/02/01 2024, doi: 10.1007/s40745-021-00364-7.

[30] P. Luangpaiboon, R. Piachat, and N. Imsap, "IMPLEMENTING THE TAGUCHI-STATISTICAL LEARNING-DEAR METHODOLOGY IN A MULTI-CRITERIA DECISION MAKING APPROACH TO BALANCE TRADE-OFFS IN EVOLUTIONARY ALGORITHM PERFORMANCE," *Science & Technology Asia*, vol. 29, no. 2, pp. 156-172, 2024, doi: 10.14456/scitechasia.2024.34.

[31] E. V. Altay, O. Altay, and Y. Özçevik, "A COMPARATIVE STUDY OF METAHEURISTIC OPTIMIZATION ALGORITHMS FOR SOLVING REAL-WORLD ENGINEERING DESIGN PROBLEMS," *CMES - Computer Modeling in Engineering and Sciences*, vol. 139, no. 1, pp. 1039-1094, 2023/12/30/ 2023, doi: https://doi.org/10.32604/cmes.2023.029404.